# On-line Bayesian Model Updating and Model Selection of a Piece-wise model for the Creep-growth rate prediction of a Nuclear component

Adolphus Lye *[1], Alice Cicirello[1,2], and Edoardo Patelli[3]

[1] *Institute for Risk and Uncertainty, University of Liverpool, United Kingdom*
[2] *Faculty of Civil Engineering and Geoscience, Delft University of Technology, The Netherlands*
[3] *Centre for Intelligent Infrastructure, University of Strathclyde, United Kingdom*

**Abstract**

This work presents an application of the recently-developed Sequential Ensemble Monte Carlo sampler in performing on-line Bayesian model updating for the Prognostics Health Management of a passive component of an Advanced Reactor. The passive component involves a stainless-steel material subjected to a thermal creep deformation whose growth rate is modelled by a continuous piece-wise model consisting of 3 models, each representing a creep-growth stage.

There are 2 investigations done in this research. For the first investigation, the model identification capability of the Sequential Monte Carlo sampler is evaluated in identifying the most probable model for each creep-growth stage. For the second investigation, the on-line Bayesian model updating procedure via the aforementioned sampler is then undertaken. In addition, a method is proposed where the model updating approach will be done for each model sequentially across the different creep-growth stage. This process involves utilising information of the boundary conditions obtained from the model output interval at the transition times to determine the prior bounds for each model parameter to be updated. This method seeks to minimise the discontinuity in the updated piece-wise model at the transition times. From there, the Remaining Useful Life analysis on the component is performed.

**Keywords**: Bayesian Model Updating, Model Selection, Uncertainty Quantification, Nuclear, Prognostics, Remaining Useful Life

## 1. Introduction

In recent years, on-line Bayesian model updating technique has been gaining popularity as a technique to address numerous problems in engineering. This involves the updating of knowledge of the inferred parameter(s) while the distinct data-sets are obtained sequentially across different times. As such, this technique is of importance in the context of Prognostics Health Management where real-time monitoring of the component's state of health is of importance for timely maintenance and Remaining Useful Life (RUL) prediction [1]. There are 2 significant advantages to such approach: 1) it does not require a complete data-set to be present in order to perform Bayesian inference; and 2) it allows for condition-based maintenance to be done rather than time-based maintenance which is more frequent and costly [1].

For the work presented in this paper, on-line Bayesian model updating is implemented to perform probabilistic model updating on a continuous piece-wise model. To the best of the authors' knowledge, such work has not been done previously which will be addressed here. This research comprises of 2 key objectives: 1) to assess and evaluate the capability of the recently-developed Sequential Ensemble Monte Carlo (SEMC) [2] sampler to identify the most probable model for the corresponding sub-domain under uncertainty; and 2) to propose a method to account for boundary conditions when determining the prior bounds for the selected inferred model parameters based on interval arithmetic [3]. The eventual goal of this research is to arrive at an approach to ensure that the updated piece-wise model captures most of the information contained by the observed data whilst ensuring minimal discontinuities between the sub-domains.

### *1.1. Bayesian Model Updating*

A well-known probabilistic model updating technique commonly used in engineering is Bayesian model updating [4]. The framework based on Bayesian inference [5]:

$$P(\boldsymbol{\theta}|\boldsymbol{D}, M) = \frac{P(\boldsymbol{\theta}|M) \cdot P(\boldsymbol{D}|\boldsymbol{\theta}, M)}{P(\boldsymbol{D}|M)} \tag{1}$$

The terms in Eq. (1) follows: $\boldsymbol{\theta}$ is the vector of the inferred epistemic parameters; $\boldsymbol{D}$ is the vector of measurements; $M$ is the mathematical model which predicts the observed $\boldsymbol{D}$ as a function of $\boldsymbol{\theta}$; $P(\boldsymbol{\theta}|M)$ is the prior distribution; $P(\boldsymbol{D}|\boldsymbol{\theta}, M)$ is the likelihood function; $P(\boldsymbol{\theta}|\boldsymbol{D}, M)$ is the posterior distribution; and $P(\boldsymbol{D}|M)$ is the evidence. Detailed explanations to the above terms are found in [6].

In the on-line Bayesian model updating framework, data is obtained sequentially at different time $t_s$ where $s$ denotes the time index. Such set-up is used to infer $\boldsymbol{\theta}$ which can be either time-invariant or time-varying. In this paper, we shall only consider the case where $\boldsymbol{\theta}$ is time-invariant. As such, assuming independence between the data obtained at different $t_s$, the posterior at a given $t_s$ is defined [7]:

$$P(\boldsymbol{\theta}|\boldsymbol{D}^{1:s}, M) \propto P(\boldsymbol{\theta}|M) \cdot \prod_{s=1}^{s_{end}} P(\boldsymbol{D}^{s}|\boldsymbol{\theta}, M) \tag{2}$$

where $s_{end}$ is the index for the terminal time.

Eq. (2), implies that $P(\boldsymbol{\theta}|\boldsymbol{D}^{1:s}, M)$ is time-varying. As such, samples have to be obtained sequentially across all $t_s$. To do this, several sampling techniques can be employed such as Kalman Filter [8], Gaussian Sum Filters [9], [10], and Sequential Monte Carlo samplers [11]. For the research work presented here, a new variant of Sequential Monte Carlo sampler, known as the Sequential Ensemble Monte Carlo (SEMC) sampler [2], will be implemented.

*E-Mail: adolphus.lye@liverpool.ac.uk

### *1.2. Review of the Sequential Ensemble Monte Carlo*

The SEMC sampler presents 2 key features: 1) the use of the Affine-invariant Ensemble sampler (AIES) in place of the Metropolis-Hastings (MH) sampler for the Markov Chain Monte Carlo (MCMC) step; and 2) an adaptive-tuning algorithm which tunes automatically the step-size parameter of the AIES [2].

#### *1.2.1. Affine-invariant Ensemble sampler*

The AIES is a MCMC algorithm developed by Goodman and Weare in 2010 which involves the use of multiple chains (i.e. an ensemble) to explore the sample space defined by the target distribution. From which, it utilises an affine-invariant stretch-move kernel to generate candidate samples $\boldsymbol{\theta}^*$ between chains contrary to the MH algorithm which utilises a proposal distribution (i.e. a Normal distribution) to generate $\boldsymbol{\theta}^*$ for one chain at a time which does not exhibit the affine-invariant property [12]. As a result, the AIES is able to sample from highly-skewed, anisotropic distributions compared to its MH counterpart. To highlight this, extensive studies have been done in [12], [13] to which readers can refer for details.

The AIES generates $N_e$ ensemble as follows: Defining the $i^{th}$ ensemble $\vec{\boldsymbol{\theta}}_i = \{\boldsymbol{\theta}_{1,i}, \boldsymbol{\theta}_{2,i}, \ldots, \boldsymbol{\theta}_{N_c-1,i}, \boldsymbol{\theta}_{N_c,i}\}$, where $N_c$ is the total number of chains; and $i = 1, \ldots, N$ is the iteration number. It needs to be noted that $N_c \geq 2 \times N_d$ where $N_d$ is the total number of inferred parameters [12]. For each iteration $i$, a given chain $k$, for $k = 1, \ldots, N_c$, is updated through the stretch-move kernel [12]:

$$\boldsymbol{\theta}_k^* = \boldsymbol{\theta}_{[k]}^* + \lambda \cdot (\boldsymbol{\theta}_{k,i}^* - \boldsymbol{\theta}_{[k]}^*) \tag{3}$$

where $\boldsymbol{\theta}_k^*$ is the candidate sample of the $k^{th}$ chain; $\boldsymbol{\theta}_{[k]}$ is a randomly chosen sample from the complementary set $\vec{\boldsymbol{\theta}}_{[k]} = \{\boldsymbol{\theta}_{1,i+1}, \ldots, \boldsymbol{\theta}_{k-1,i+1}, \boldsymbol{\theta}_{k+1,i}, \ldots, \boldsymbol{\theta}_{N_c,i}\}$; and $\lambda$ is real-valued scalar proposal stretch factor. $\lambda$ is a random variable following a proposal distribution $g(\lambda)$:

$$g(\lambda) = \begin{cases} \frac{1}{2\cdot(\sqrt{u} - \frac{1}{\sqrt{u}})} \cdot \frac{1}{\sqrt{\lambda}} & \text{if } \lambda \in [\frac{1}{u}, u] \\ 0 & \text{otherwise} \end{cases} \tag{4}$$

where $u \geq 1$ is the user-defined step-size auxiliary parameter of the AIES sampler. From there, $\boldsymbol{\theta}_k^*$ is accepted with probability $\alpha_k$:

$$\alpha_k = min\left[1,\ \lambda^{N_d-1} \cdot \frac{P(\boldsymbol{\theta}_k^*|\boldsymbol{D}^{1:s}, M)}{P(\boldsymbol{\theta}_{k,i}|\boldsymbol{D}^{1:s}, M)}\right] \tag{5}$$

This process is repeated for all $N_c$ chains upon which when this is done, the algorithm proceeds to iteration $i = i + 1$ and repeats the above procedure until $i = N_e$.

#### *1.2.2. Adaptive Tuning Algorithm*

The adaptive tuning algorithm was proposed in [13] to allow for the automatised tuning of $u$ which, in turn, helps to control the acceptance-rates of the sampler at each iteration $j$. The algorithm works as such: At $j = 1$, an initial value of $u$ is set. Although the recommended value is 2, as this is the "optimal" value for most problems [12], this initial value can vary depending on the complexity of the problem and the number of parameters to be inferred. From this initial value, the nominal step-size $u_{nom}$ is computed after the MCMC step:

$$u_{nom} = u^j \cdot exp\left[\alpha^j - \alpha_{tr}\right] \tag{6}$$

where $\alpha^j$ is the overall acceptance rate of the AIES sampler at iteration $j$ of the SEMC sampler, while $\alpha_{tr}$ is the target acceptance rate defined as [14]:

$$\alpha_{tr} = \frac{0.21}{N_d} + 0.23 \tag{7}$$

If $u_{nom} > 1$, set $u^{j+1} = u_{nom}$. Else, set $u^{j+1} = 1.01$.

#### *1.2.3. SEMC Sampling Algorithm*

The SEMC algorithm generates $N$ samples from the posterior as such [2]:

1. Initialise sampler (i.e. $j = 0$). Sample $N$ samples of $\boldsymbol{\theta}_i^{j+1} \sim P(\boldsymbol{\theta}|M)$ for $i = 1, \ldots, N$;
2. Set $j = 1$ and $u^{j=1} = 2$.
3. Compute the weights $\hat{w}_i^j = \frac{P(\boldsymbol{D}^j|\theta_i^j, M)}{\sum_{i=1}^N P(\boldsymbol{D}^j|\theta_i^j, M)}$;
4. Compute $N_{eff} = \frac{1}{\sum_{i=1}^N \left(\hat{w}_i^j\right)^2}$;
5. If $N_{eff} < \frac{N}{2}$, resample $N$ $\boldsymbol{\theta}_i^j \sim \hat{w}_i^j$ and set $\hat{w}_i^j = \frac{1}{N}$.
6. Resample $N$ samples of $\boldsymbol{\theta}_i^j \sim \hat{w}_i^j$ and set them as initial ensemble $\vec{\boldsymbol{\theta}}_1$. Generate $\vec{\boldsymbol{\theta}}_2$ via 1 iteration of the AIES algorithm according to $P(\boldsymbol{\theta}^j|\boldsymbol{D}^{1:j}, M)$;
7. Compute $u_{nom}$ via Eq. (6).
8. If $u_{nom} > 1$, set $u^{t+1} = u_{nom}$. Else, set $u^{t+1} = 1.01$;
9. Set $P(\boldsymbol{\theta}^j|\boldsymbol{D}^{1:j}, M)$ as the new prior PDF and $\boldsymbol{\theta}_i^j$ as the new prior samples;
10. Compute evidence: $P(\boldsymbol{D}^{1:j}|M) \approx \frac{1}{N} \prod_{m=1}^j \sum_{i=1}^N P(\boldsymbol{D}^m|\boldsymbol{\theta}_i^m, M)$;
11. Set $j = j + 1$ and repeat Steps 3 to 10 until $j = j_{end}$ (Terminal iteration).

## 2. Case Study

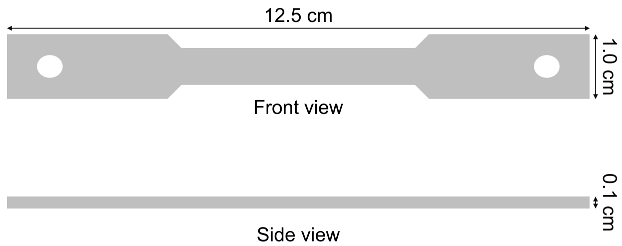


**Figure 1.** Schematic diagram of the Advanced Reactor passive component with its corresponding dimensions. Image adopted from [15].

The set-up involves an Advanced Reactor passive component whose schematics is illustrated in Figure 1. In [15], the effect of thermal creep degradation of the component is studied for the purpose of assessing its Prognostics Health Management (PHM) framework. To do so, the literature presented a numerical study using synthetic data of creep-growth rate $\frac{d\epsilon}{dt}$, in units of percent strain, generated from 3 different models representing the corresponding creep-growth stage: 1) $\hat{M}_1$ (Primary stage); 2) $\hat{M}_2$ (Secondary stage); and 3) $\hat{M}_3$ (Tertiary stage). These models are defined respectively following [15]:

$$\hat{M}_1(t) = 1 - exp\,(-0.40 \cdot t)\,, \text{ for } 0 \leq t \leq 6 \tag{8}$$

$$\hat{M}_2(t) = 0.07 \cdot t + 0.75, \text{ for } 6 < t \leq 24 \tag{9}$$

$$\hat{M}_3(t) = 3.52e{-}04 \cdot t^3 - 1e{-}05 \cdot t^2 - 0.63 \cdot t + 12.93, \text{ for } t > 24 \tag{10}$$

where $t$ is in $hrs$.

The synthetic data-set $\boldsymbol{D}(t)$ is obtained at $t = \{0, 2, 3, 4, 7, 11, 15, 19, 23, 26, 27, 28, 30\}$ $hrs$. For each $t$, the corresponding $\boldsymbol{D}(t)$ is obtained following [15]:

$$\boldsymbol{D}(t) = \hat{M}(t) + \varepsilon, \text{ for } \varepsilon \sim N(0, 0.1^2) \tag{11}$$

where $\hat{M}(t)$ is the creep-growth model (i.e. see Eq. (8) to (10)), and $\varepsilon$ is the simulated "measurement error" term. The resulting synthetic data is illustrated in Figure 2.

There are 2 investigations involved in this case-study: 1) to evaluate the capability of the SEMC sampler to identify the appropriate creep-growth model for each creep-growth stage; and 2) to propose a methodology for the on-line model updating of the piece-wise creep-growth rate model.

## 3. Investigation 1: Model Identification

To identify the most probable model for each creep-growth stage under uncertainty, at a given $t_s$, the model probability posterior $P(M|\boldsymbol{D}^{1:s})$ is used as the metric. For a given $v^{th}$ model $M_v$, its model probability posterior computed as [16]:

$$P(M_v|\boldsymbol{D}^{1:s}) = \frac{P(M_v) \cdot P(\boldsymbol{D}^{1:s}|M_v)}{P(\boldsymbol{D}^{1:s})} \tag{12}$$

where $P(M_v)$ is the prior probability of model $M_v$, $P(\boldsymbol{D}^{1:s}|M_v)$ is the evidence computed from the SEMC sampler (i.e. see Section 1.2.3); and $P(\boldsymbol{D}^{1:s}) = \sum_v P(M_v) \cdot P(\boldsymbol{D}^{1:s}|M_v)$ is the normalisation constant.

In this investigation, it will be assumed that we have no a priori knowledge that the creep-growth rate model is piece-wise. As such, the approach would involve the use of 5 different possible models, each defined for $t \in [0, 30]$ $hrs$ as follows:

$$M_1(t) = \theta_2 \cdot [1 - exp(-\theta_1 \cdot t)] \tag{13}$$

$$M_2(t) = \theta_2 \cdot t + \theta_1 \tag{14}$$

$$M_3(t) = \theta_4 \cdot t^3 + \theta_3 \cdot t^2 + \theta_2 \cdot t^1 + \theta_1 \tag{15}$$

$$M_4(t) = \theta_2 \cdot exp(\theta_1 \cdot t) \tag{16}$$

$$M_5(t) = exp(\theta_2 \cdot t^2 + \theta_1 \cdot t) \tag{17}$$

where $\theta_1$ to $\theta_4$ are the epistemic model parameters. Models $M_4$ and $M_5$ are introduced as potential functions, in addition to model $M_3$, to model the creep-growth rate in Stage III. There are 2 reasons for this: 1) Model $M_3$ is a cubic function which could be too specific of a choice of function to model Stage III of creep-growth rate; and 2) Model $M_3$ introduces more (and possibly unnecessary) inferred parameters to infer which makes it relatively complex compared to models $M_4$ and $M_5$ which involve less inferred parameters and would less-likely over-fit the data in Stage III (i.e. Occam's razor [17]).

Another assumption in this investigation is that we do not have any a priori information on the prior probability of model $M_v$, for $v = 1, \ldots, 5$. As such, it will be treated that all models $M_v$ are equally probable. Hence, Eq. (12) is simplified as:

$$P(M_v|\boldsymbol{D}^{1:s}) = \frac{P(\boldsymbol{D}^{1:s}|M_v)}{\sum_v P(\boldsymbol{D}^{1:s}|M_v)} \tag{18}$$

### *3.1. Bayesian Inference Set-up*

For each of the given model in Eq. (13) to (17), its corresponding epistemic model parameters are assigned a Uniform prior with the respective bounds presented in Table 1. In addition, the measurement error term $\sigma$ will also be inferred given the lack of prior knowledge and is assigned a Uniform prior with the interval: $[0.001, 1]$ %.

**Table 1.** Uniform prior bounds for the respective inferred model parameters.

| Model | $\theta_1$ | $\theta_2$ | $\theta_3$ | $\theta_4$ |
|---|---|---|---|---|
| $M_1$ | $[-5, 5]$ | $[0, 5]$ | – | – |
| $M_2$ | $[-5, 5]$ | $[0, 5]$ | – | – |
| $M_3$ | $[0, 15]$ | $[-1, 1]$ | $[-0.1, 0.1]$ | $[0, 0.01]$ |
| $M_4$ | $[0.01, 1]$ | $[0.01, 50]$ | – | – |
| $M_5$ | $[0, 1]$ | $[-5, 5]$ | – | – |

The likelihood function at $t_s$, given model $M_v$, is modelled as a Normal distribution [6]:

$$P(\boldsymbol{D}^s|\boldsymbol{\theta}, M_v) = \frac{1}{\sigma \cdot \sqrt{2\pi}} exp\left[-\frac{(\boldsymbol{D}^s - M_v(\boldsymbol{\theta}))^2}{2 \cdot \sigma^2}\right] \tag{19}$$

The SEMC sampler is implemented for each $M_v$ with the number of samples set at $N = 1000$.

### *3.2. Results and Discussions*

The resulting $P(M_v|\boldsymbol{D}^{1:j})$ is computed using Eq. (18) and the numerical results are presented in Table 2 while corresponding graphical plots are illustrated in Figure 3.

From Figure 3, it is observed that the SEMC sampler is able to identify models $M_1$ and $M_2$ being the most probable models for creep-growth Stages I and II respectively. The results are consistent with the true set-up described in Section 2 as well as the results obtained in the work by Ramuhalli *et. al* [15]. However, from iteration $j = 9$ onwards, it can be seen that model $M_2$ is the most probable model to describe Stage III of creep-growth rate with a probability close to 1. In addition, models $M_3$, $M_4$, and $M_5$ are observed to have probabilities close to 0 which is mathe-

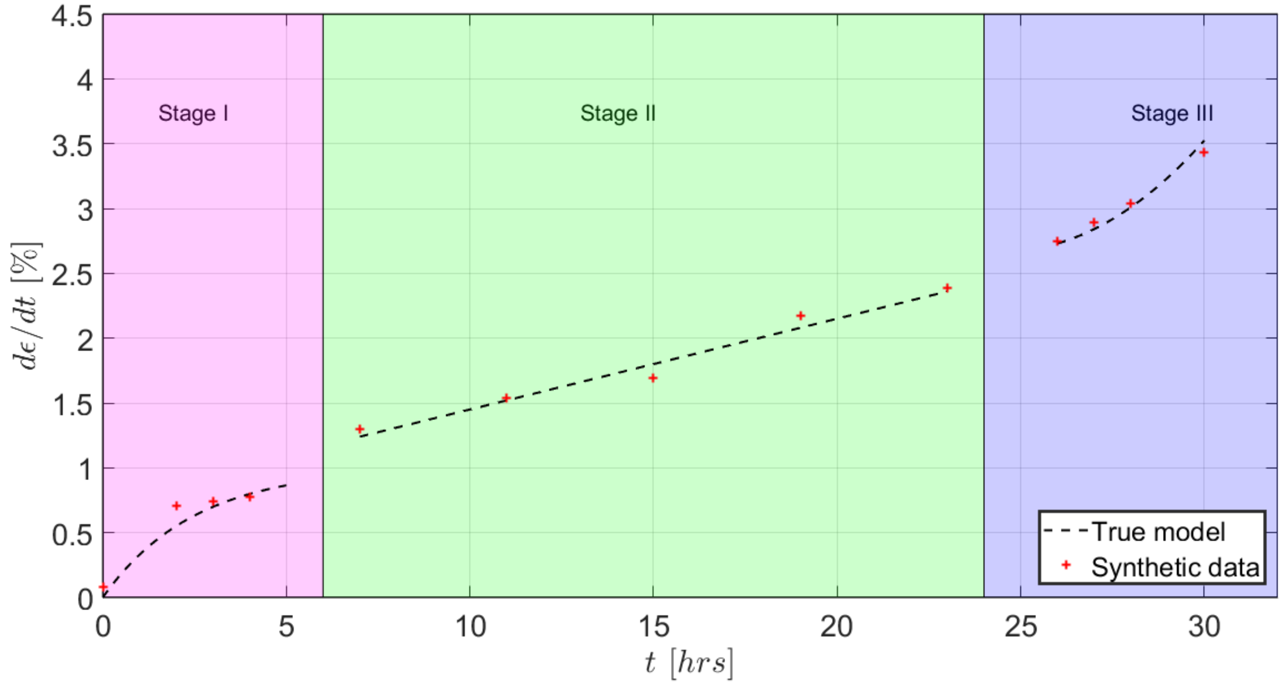


**Figure 2.** Synthetic data of creep-strain growth rate, $\frac{d\epsilon}{dt}$, against time, $t$.

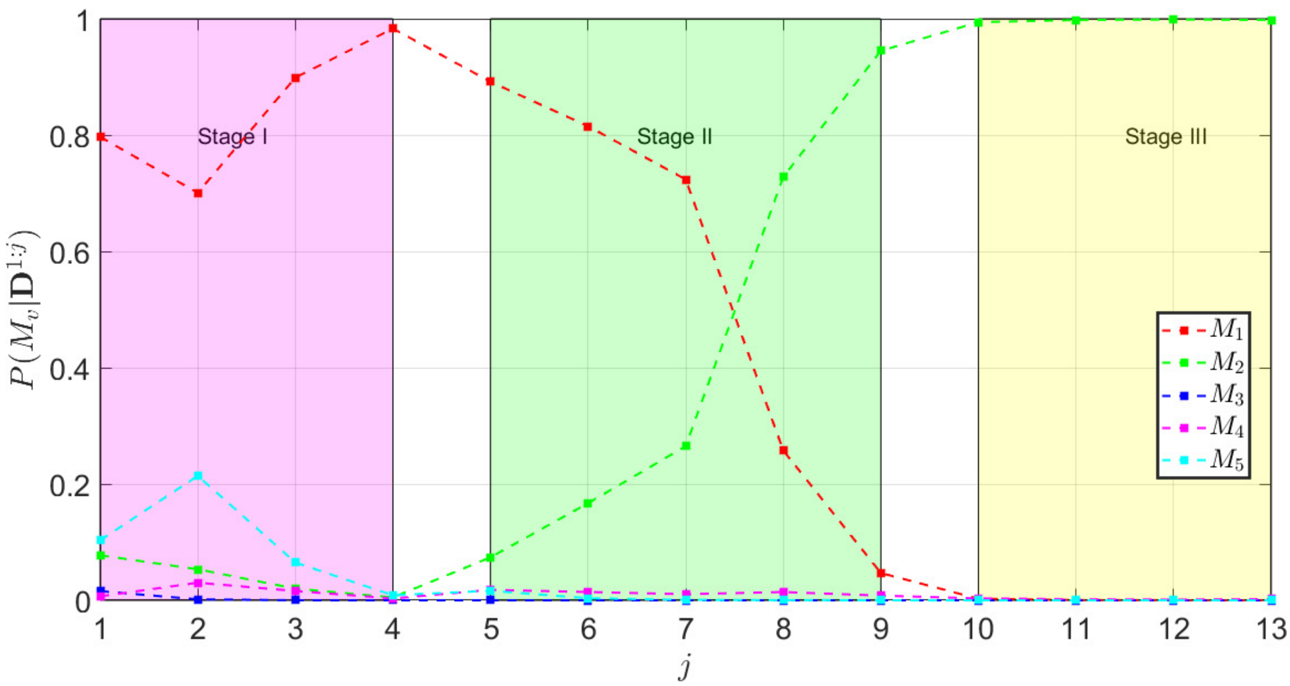


**Figure 3.** Results of $P(M_\nu|\boldsymbol{D}^{1:j})$ for all models $M_\nu$ across iterations $j$.

matically inconsistent. This is especially so for the case of model $M_3$ to which the result also disagrees to the set-up described in Section 2.

The above observations imply that the SEMC sampler is able to effectively identify the most probable models up to the $9^{th}$ data point (i.e. iteration $j = 9$). The reason behind the failure of the SEMC sampler to correctly identify the most appropriate model from the $10^{th}$ data point onwards is due to the posterior at iteration $j = 9$ (i.e. $P(\boldsymbol{\theta}|\boldsymbol{D}^{1:9}, M_\nu)$) being dominated by $P(\boldsymbol{D}^j|\boldsymbol{\theta}, M_\nu)$ obtained from iterations $j = 1$ to $j = 9$. As a result, any further information contained in $P(\boldsymbol{D}^j|\boldsymbol{\theta}, M_\nu)$ from $j = 10$ onwards would not significantly update the posterior obtained from the iteration before. This, in turn, leads to the data in Stage III being ineffective in providing information towards the identification of either models $M_3$, $M_4$, or $M_5$.

**Table 2.** Numerical results of $P(M_v|\boldsymbol{D}^{1:j})$ obtained at each iteration $j$ for the corresponding model $M_v$.

| $j$ | $M_1$ | $M_2$ | $M_3$ | $M_4$ | $M_5$ |
|---|---|---|---|---|---|
| 1 | 0.797 | 0.077 | 0.000 | 0.007 | 0.103 |
| 2 | 0.701 | 0.053 | 0.000 | 0.030 | 0.214 |
| 3 | 0.899 | 0.020 | 0.000 | 0.016 | 0.065 |
| 4 | 0.983 | 0.005 | 0.000 | 0.003 | 0.009 |
| 5 | 0.892 | 0.074 | 0.000 | 0.018 | 0.017 |
| 6 | 0.815 | 0.167 | 0.000 | 0.014 | 0.004 |
| 7 | 0.724 | 0.265 | 0.000 | 0.011 | 0.000 |
| 8 | 0.258 | 0.728 | 0.000 | 0.014 | 0.000 |
| 9 | 0.047 | 0.945 | 0.000 | 0.008 | 0.000 |
| 10 | 0.003 | 0.994 | 0.000 | 0.003 | 0.000 |
| 11 | 0.000 | 0.998 | 0.000 | 0.002 | 0.000 |
| 12 | 0.000 | 0.999 | 0.000 | 0.001 | 0.000 |
| 13 | 0.000 | 0.998 | 0.000 | 0.002 | 0.000 |

To address this issue, the procedure is repeated involving only the data in Stage III. Considering that the results from the previous analysis have concluded that model $M_1$ is the most probable model given the data in Stage I, it will be excluded from this round of the analysis. For models $M_2$ and $M_3$, inferred model parameters are assigned a Uniform prior with the respective bounds as per in Table 1. For the case of models $M_4$ and $M_5$, the inferred model parameters are also assigned a Uniform prior with the following bounds presented in Table 3. It needs to be noted that the logarithmic scale is used for the bounds to provide numerical stability.

**Table 3.** Uniform prior bounds for the respective inferred model parameters of models $M_4$ and $M_5$.

| Model | $log(\theta_1)$ | $log(\theta_2)$ |
|---|---|---|
| $M_4$ | $[-4, -1.9]$ | $[-4, -1]$ |
| $M_5$ | $[-10, -3]$ | $[-3, -2]$ |

The numerical results to $P(M_v|\boldsymbol{D}^{1:j})$ across the iterations $j$ for the respective models $M_v$ are presented in Table 4 while the resulting graphical plots are illustrated in Figure 4. From the figure, it is evident that the model posterior probability is consistently the highest for model $M_4$ instead of $M_3$ which substantiates the hypothesis set-forth by Occam's razor.

**Table 4.** Numerical results of $P(M_v|\boldsymbol{D}^{1:j})$ obtained at each iteration $j$ for the corresponding model $M_v$.

| $j$ | $M_2$ | $M_3$ | $M_4$ | $M_5$ |
|---|---|---|---|---|
| 1 | 0.048 | 0.080 | 0.832 | 0.041 |
| 2 | 0.070 | 0.073 | 0.850 | 0.008 |
| 3 | 0.163 | 0.036 | 0.799 | 0.001 |
| 4 | 0.114 | 0.033 | 0.852 | 0.000 |

Hence, from the results presented in this section, it can be concluded that the following models are the most probable to represent the data for the corresponding creep-growth Stage: I) Model $M_1$; II) Model $M_2$; and III) Model $M_4$. These findings will be used to perform the Bayesian model updating of the piece-wise creep-growth rate model to which the procedure is described in Section 4.

## 4. Investigation 2: Model Updating

In updating the piece-wise creep-growth rate model, the objective is to minimise discontinuity in the updated model between the different creep-growth stages. To achieve this, the following set of procedures are proposed and implemented: 1) For Stage I, model $M_1$ is updated with information from the data in Stage I as well as the first data in Stage II (i.e. at $t = 7$ $hrs$); 2) For Stage II, model $M_2$ is updated with information from the data in Stage II, the last data in Stage I (i.e. at $t = 4$ $hrs$), and the first data in Stage III (i.e. at $t = 26$ $hrs$); and 3) For Stage III, model $M_4$ is updated with information from the data in Stage III as well as the last data in Stage II (i.e. at $t = 23$ $hrs$).

In addition to the above procedures, boundary conditions are introduced when determining the prior bounds on the inferred model parameters. This will be done as follows: 1) Upon updating model $M_1$, the bounds on the probabilistic model output at $t = 6$ $hrs$, denoted as $[\underline{m_1}, \overline{m_1}]$, are obtained; 2) For a given set of Uniform prior bounds on $\theta_2$ for model $M_2$, denoted as $[\underline{\theta_2}, \overline{\theta_2}]_{M_2}$, the Uniform prior bounds on $\theta_1$ is computed following:

$$[\underline{\theta_1}, \overline{\theta_1}]_{M_2} = [\underline{m_1}, \overline{m_1}] - [\underline{\theta_2}, \overline{\theta_2}]_{M_2} \cdot 6 \qquad (20)$$

3) Similarly, upon updating model $M_2$, the bounds on the probabilistic model output at $t = 24$ $hrs$, denoted as $[\underline{m_2}, \overline{m_2}]$, are obtained; 4) For a given set of Uniform prior bounds on $\theta_1$ for model $M_4$, denoted as $[\underline{\theta_1}, \overline{\theta_1}]_{M_4}$, the Uniform prior bounds on $\theta_2$ is computed following:

$$[\underline{\theta_2}, \overline{\theta_2}]_{M_4} = \frac{[\underline{m_2}, \overline{m_2}]}{exp\left([\underline{\theta_1}, \overline{\theta_2}]_{M_1} \cdot 24\right)} \qquad (21)$$

### 4.1. Bayesian Inference Set-up

Based on the methodology described in Section 4, the Uniform prior bounds of the inferred model parameters for the respective models are presented in Table 5. Note that the logarithmic scale is used for the inferred model parameters for model $M_4$ to provide numerical stability.

**Table 5.** Uniform prior bounds for the respective inferred model parameters.

| Model | Bounds |
|---|---|
| $M_1$ | $\theta_1 \in [0, 2];\ \theta_2 \in [0, 2]$ |
| $M_2$ | $\theta_1 \in [\underline{\theta_1}, \overline{\theta_1}]_{M_2};\ \theta_2 \in [0, 1]$ |
| $M_4$ | $log(\theta_1) \in [-4, 0];\ log(\theta_2) \in log\left([\underline{\theta_2}, \overline{\theta_2}]_{M_4}\right)$ |

As per in Section 3.1, the measurement error term $\sigma$ will also be inferred with its aforementioned Uniform prior bounds and the Normal distribution is assigned as the likelihood function (i.e. see Eq. (19)).

The SEMC sampler is implemented to perform Bayesian

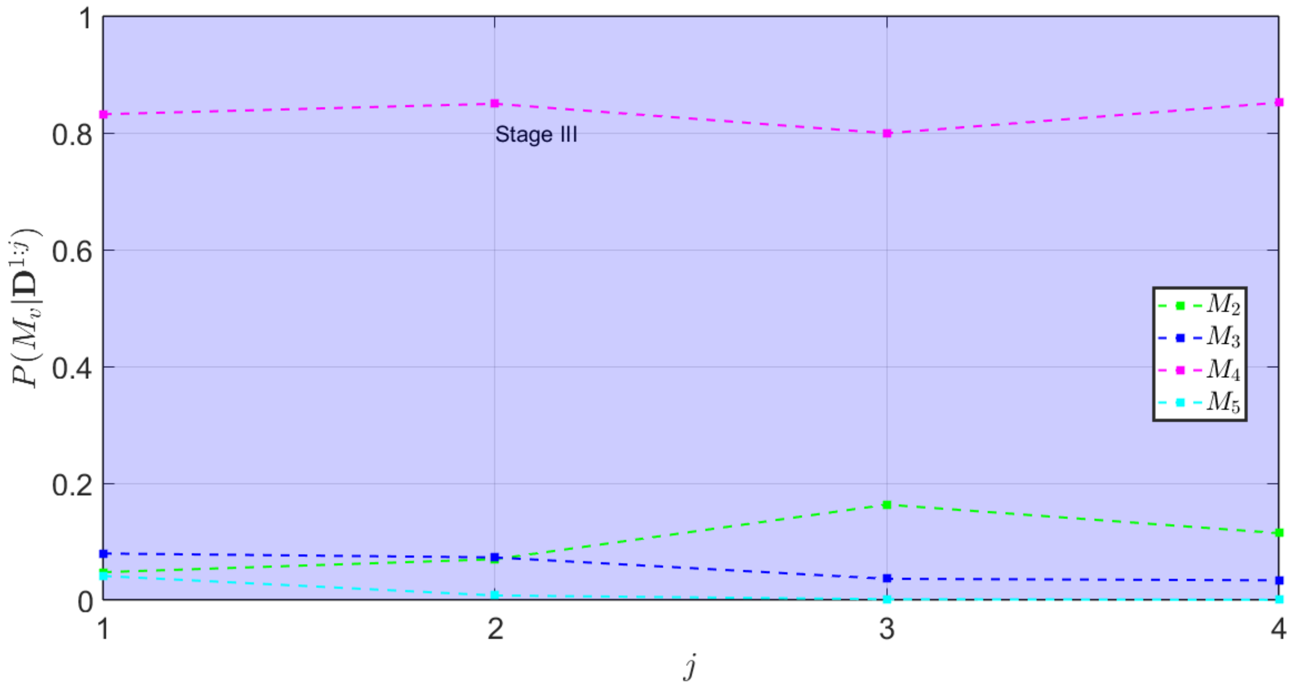


**Figure 4.** Results of $P(M_v|\boldsymbol{D}^{1:j})$ for models $M_2$ to $M_5$ across iterations $j$.

model updating on each model with a sample size of $N$ = 1000.

### *4.2. Results and Discussions*

The resulting graphical plots for the updated piece-wise creep-growth rate model are illustrated in Figure 5. From the figure, it can be observed that the updated piece-wise model generally encompasses the synthetic data points as well as the true models for the respective creep-growth rate stage. In addition, the updated piece-wise model is generally smooth and continuous except at $t = 6$ $hrs$ and $t = 24$ $hrs$ where small degrees of discontinuity can be seen. This indicates that the Bayesian model updating procedure, along with the proposed methodologies presented in Section 4, are effective to a large extent.

Following this, the analysis on the RUL of the Advanced Reactor component is conducted at $t = \{7, 11, 15, 19, 23, 26, 27, 28, 30\}$ $hrs$ with the end-of-life of the component is set at $t = 30$ $hrs$ [15]. The mean RUL at each $t$ is computed by first considering the value of $\frac{d\epsilon}{dt}$ for that particular $t$. From there, the output distribution of $t$ from the updated piece-wise model given $\frac{d\epsilon}{dt}$ is obtained from which the mean RUL is derived. From the output distribution of $t$, the 90 % Credible Interval (CI) of the RUL estimates can be generated based on the interval obtained by taking its alpha-cut at $\alpha = 0.05$ level [18]. The numerical results to the mean RUL and its 90 % CI for the respective $t$ are presented in Table 6 while its graphical plots are illustrated in Figure 6.

From Table 6 and Figure 6, it can be seen that in most cases, the 90 % CI of the RUL estimates includes the true RUL which verifies the Bayesian model updating results and validates the proposed methodologies. It can be noticed, however, the significantly larger 90 % CI of the RUL estimate at $t = 23$ $hrs$. The reason behind this due to the discontinuity in the updated piece-wise creep-growth rate model at $t = 24$ $hrs$ which results in the bounds being artificially wider.

**Table 6.** Results of the RUL estimates, along with its corresponding 90 % CI, for the respective $t$.

| Time $[hrs]$ | True RUL $[hrs]$ | Mean RUL $[hrs]$ | 90 % CI $[hrs]$ |
|---|---|---|---|
| 7 | 23 | 21.09 | $[20.49, 21.73]$ |
| 11 | 19 | 18.21 | $[17.69, 18.76]$ |
| 15 | 15 | 16.28 | $[15.68, 16.87]$ |
| 19 | 11 | 10.47 | $[9.62, 11.20]$ |
| 23 | 7 | 7.66 | $[4.04, 8.85]$ |
| 26 | 4 | 3.90 | $[3.58, 4.45]$ |
| 27 | 3 | 2.95 | $[2.72, 3.25]$ |
| 28 | 2 | 2.08 | $[1.76, 2.37]$ |
| 30 | 0 | 0.09 | $[0, 0.42]$ |

## 5. Conclusion

This paper has demonstrated the application of the SEMC sampler for on-line Bayesian model updating of a continuous piece-wise model in the context of the creep-growth rate model for an Advanced Reactor passive component. This is achieved through 2 investigations: 1) the identification of the corresponding model for each creep-growth rate stage; and 2) the introduction of the appropriate boundary conditions at the model transition times (i.e. at $t = 6$ $hrs$ and $t = 24$ $hrs$) for the Bayesian model updating procedure.

For the first investigation, the SEMC sampler serves to

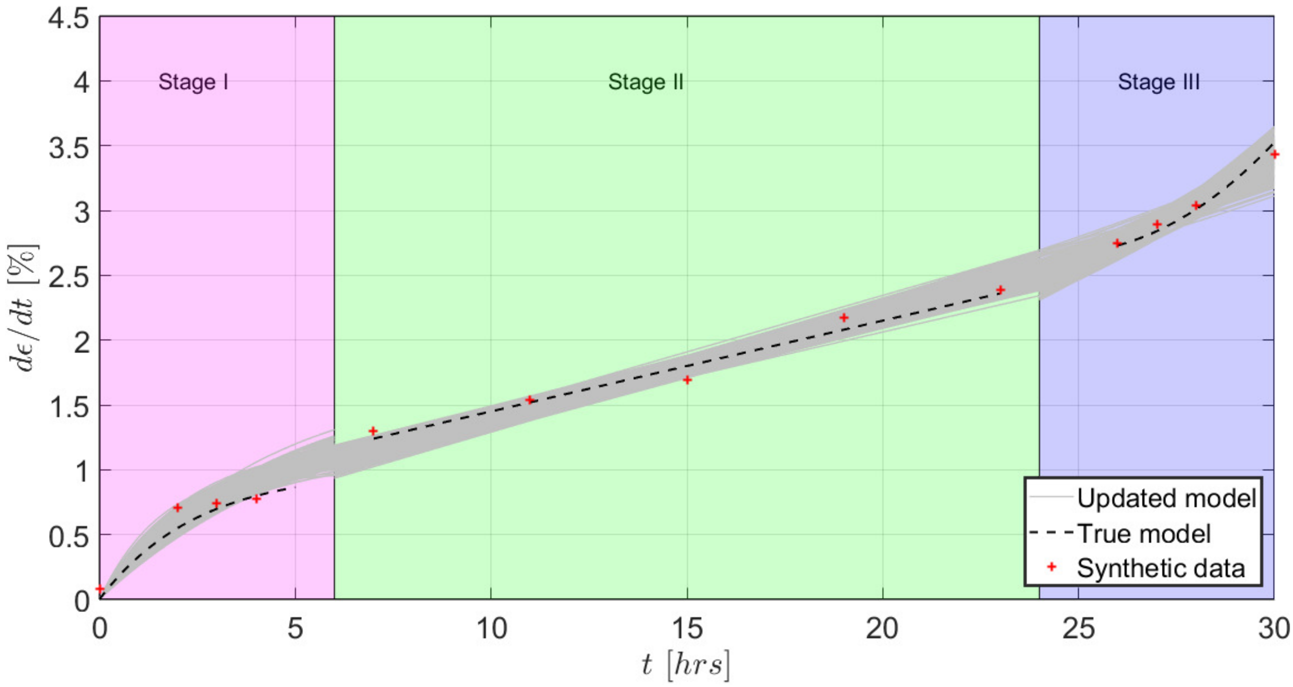


**Figure 5.** Graphical plots illustrating the updated piece-wise creep-growth model with reference to the synthetic data and the true models.

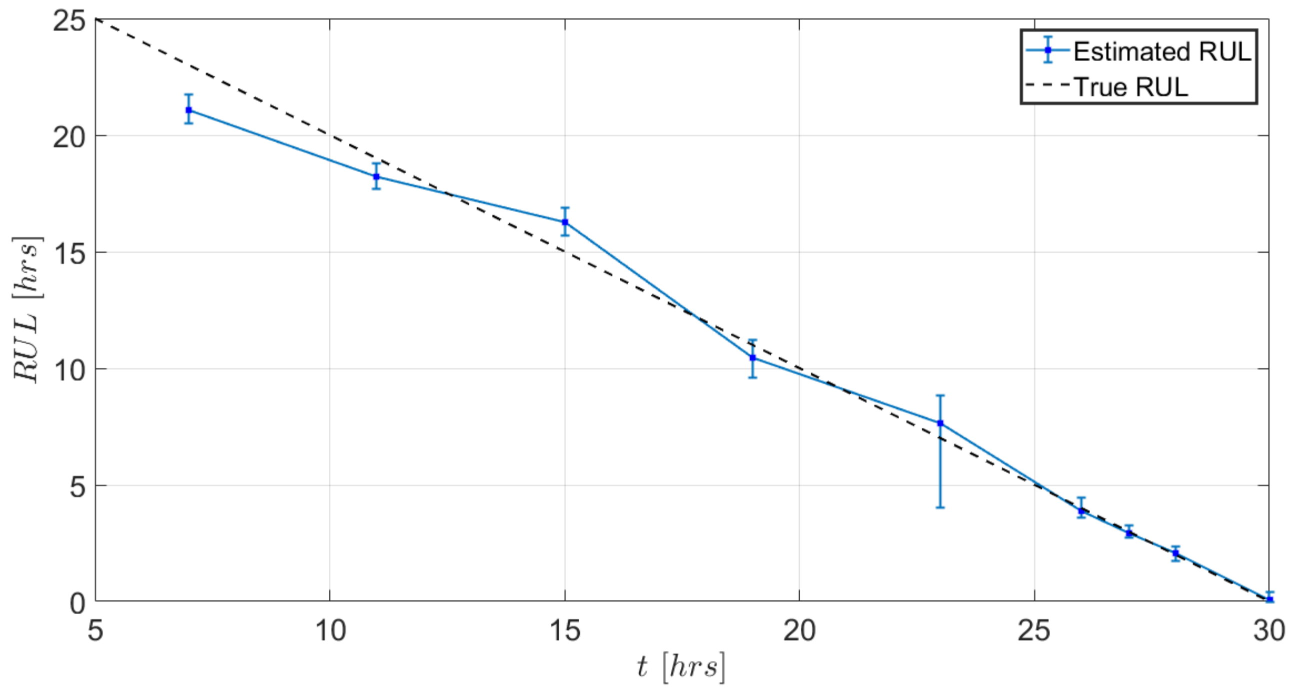


**Figure 6.** Graphical plots illustrating the estimated RUL at $t = \{7, 11, 15, 19, 23, 26, 27, 28, 30\}$ $hrs$ along with its corresponding 90 % CI.

facilitate the computation of $P(M_v|\boldsymbol{D}^{1:s})$ to determine the most probable model for the respective creep-growth stage. Simultaneously, the investigation also serves to evaluate the capability of the SEMC sampler to identify the most probable model under such settings. The results shown that the sampler was able to identify the most probable model for the respective creep-growth stages up to Stage II at $t = 24$ $hrs$. In addition, for Stage III creep-growth rate, it was found that the exponential model in Eq. (16) was the most probable model despite the true model being described by a cubic equation in Eq. (15) due to a reduced number of inferred parameters which not only simplifies the model assumptions, but also eliminates the problem of over-fitting the data.

For the second investigation, a method of determining prior bounds for the inferred model parameters is proposed. This involves using information of the model output bounds at the model transition times to introduce constraints on the prior bounds of the selected inferred model parameters which resulted in the reduction in the degree of model discontinuity at those transition times. From there, the Remaining Useful Life analysis was performed where results show that in general, the interval estimates based on the 90 % credible interval mostly encompass the true values of the remaining lifetime of the component as shown in Figure 6. This observation, along with the resulting updated creep-growth rate model encompassing most of the synthetic data points as shown in Figure 5, provide strong verification towards the proposed methodology to perform Bayesian model updating on a piece-wise model.

As an extension to this work, the following investigations need to be done: 1) to devise methods to improve the performance of the SEMC sampler in its model identification performance; 2) to look into methods to help further reduce the discontinuities at the model transition times for piece-wise continuous models; and 3) to consider the case where data is obtained at irregular intervals compared to the study presented here.

The MATLAB codes to the SEMC sampler and the case study presented in this paper are available on GitHub: `https://github.com/Adolphus8/Sequential_Ensemble_Monte_Carlo.git`


## Acknowledgment

The author would like to acknowledge the gracious funding from the Singapore Nuclear Research and Safety Initiatives (SNRSI), under the National Research Foundation Singapore, without which this research study would not have been possible.


## References


[1] R. M. Meyer, J. B. Coble, and P. Ramuhalli, "Requirements for prognostic health management of passive components in advanced small modular reactors," *In the Proceedings of the 2013 IEEE Conference on Prognostics and Health Management (PHM)*, pp. 1–8, 2013. DOI: 10.1109/ICPHM.2013.6621425.

[2] A. Lye, A. Cicirello, and E. Patelli, "On-line Bayesian Inference for Structural Health Monitoring under Model Uncertainty using Sequential Ensemble Monte Carlo," *In the Proceedings of the 13th International Conference on Structural Safety and Reliability*, vol. 1, 2022.

[3] H. Dawood, *Theories of Interval Arithmetic: Mathematical Foundations and Applications*. LAP Lambert Academic Publishing, 2011.

[4] A. Lye, A. Cicirello, and E. Patelli, "A Review of Stochastic Sampling Methods for Bayesian Inference Problems," *In the Proceedings of the 29th European Safety and Reliability Conference*, vol. 1, pp. 1866–1873, 2019. DOI: 10.3850/978-981-11-2724-3_1087-cd.

[5] J. L. Beck and L. S. Katafygiotis, "Updating models and their uncertainties. I: Bayesian statistical framework," *Journal of Engineering Mechanics*, vol. 124, pp. 455–461, 1998. DOI: 10.1061/(asce)0733-9399(1998)124:4(455).

[6] A. Lye, A. Cicirello, and E. Patelli, "Sampling methods for solving Bayesian model updating problems: A tutorial," *Mechanical Systems and Signal Processing*, vol. 159, p. 107 760, 2021. DOI: 10.1016/j.ymssp.2021.107760.

[7] P. L. Green and S. Maskell, "Estimating the parameters of dynamical systems from Big Data using Sequential Monte Carlo samplers," *Mechanical Systems and Signal Processing*, vol. 1, pp. 379–396, 2017. DOI: 10.1016/j.ymssp.2016.12.023.

[8] A. Lund, S. J. Dyke, W. Song, and I. Bilionis, "Identification of an experimental nonlinear energy sink device using the unscented Kalman filter," *Mechanical Systems and Signal Processing*, vol. 136, p. 106 512, 2020. DOI: 10.1016/j.ymssp.2019.106512.

[9] X. Wang, Q. Pan, Y. Liang, and H. Li, "Gaussian sum approximation filter for nonlinear dynamic time-delay system," *Nonlinear Dynamics*, vol. 82, pp. 501–517, 2015. DOI: 10.1007/s11071-015-2171-5.

[10] A. Lye, A. Gray, and E. Patelli, "Identification of Time-varying parameters using Variational Bayes-Sequential Ensemble Monte Carlo Sampler," *In the Proceedings of the 31st European Safety and Reliability Conference*, vol. 1, 2021. DOI: 10.3850/978-981-18-2016-8_081-cd.

[11] H. Rozas, F. Jaramillo, A. Perez, D. Jimenez, M. E. Orchard, and K. Medjaher, "A method for the reduction of the computational cost associated with the implementation of particle-filter-based failure prognostic algorithms," *Mechanical Systems and Signal Processing*, vol. 135, p. 106 421, 2020. DOI: 10.1016/j.ymssp.2019.106421.

[12] J. Goodman and J. Weare, "Ensemble samplers with affine invariance," *Communications in Applied Mathematics and Computational Science*, vol. 5, pp. 65–80, 2010. DOI: 10.2140/camcos.2010.5.65.

[13] A. Lye, A. Cicirello, and E. Patelli, "An efficient and robust sampler for Bayesian inference: Transitional Ensemble Markov Chain Monte Carlo," *Mechanical Systems and Signal Processing*, vol. 167, p. 108 471, 2022. DOI: 10.1016/j.ymssp.2021.108471.

[14] G. O. Roberts and J. S. Rosenthal, "Optimal scaling for various Metropolis-Hastings algorithms," *Statistical Science*, vol. 16, pp. 351–367, 2001. DOI: 10.1214/ss/1015346320.

[15] P. Ramuhalli, S. Roy, E. H. Hirt, *et al.*, "Component-level prognostics health management framework for passive components - advanced reactor technology milestone: M2at-15pn2301043," 2015. DOI: 10.2172/1339925.

[16] X. Guan, R. Jha, and Y. Liu, "Model selection, updating, and averaging for probabilistic fatigue damage prognosis," *Structural Safety*, vol. 33, pp. 242–249, 2011. DOI: 10.1016/j.strusafe.2011.03.006.

[17] A. Blumer, A. Ehrenfeucht, D. Haussler, and M. K. Warmuth, "Occam's Razor," *Information Processing Letters*, vol. 24, pp. 377–380, 1987. DOI: 10.1016/0020-0190(87)90114-1.

[18] J. Mockor, "A-cuts and models of fuzzy logic," *International Journal of General Systems*, vol. 42, pp. 67–78, 2013. DOI: 10.1080/03081079.2012.710438.